Journal of Experimental Botany, Vol. 61, No. 4, pp. 969–981, 2010
doi:10.1093/jxb/erp367 Advance Access publication 18 December, 2009
This paper is available online free of all access charges (see http://jxb.oxfordjournals.org/open_access.html for further details)

Journal of Experimental Botany
www.jxb.oxfordjournals.org

RESEARCH PAPER

The tobacco MAP215/Dis1-family protein TMBP200 is required for the functional organization of microtubule arrays during male germline establishment

Sung Aeong Oh[1,2], Madhumita Das Pal[1], Soon Ki Park[2], James Andrew Johnson[1] and David Twell[1,*]

[1] Department of Biology, University of Leicester, University Road, Leicester LE1 7RH, UK
[2] Division of Plant Biosciences, Kyungpook National University, Daegu 702-701, South Korea

* To whom correspondence should be addressed: E-mail: twe@leicester.ac.uk

Received 8 September 2009; Revised 9 November 2009; Accepted 18 November 2009

Abstract

The haploid microspore division during pollen development in flowering plants is an intrinsically asymmetric division which establishes the male germline for sexual reproduction. Arabidopsis *gem1* mutants lack the male germline as a result of disturbed microspore polarity, division asymmetry, and cytokinesis and represent loss-of-function mutants in *MOR1/GEM1,* a plant orthologue of the conserved MAP215/Dis1 microtubule associated protein (MAP) family. This provides genetic evidence for the role of MAP215/Dis1 in the organization of gametophytic microtubule arrays, but it has remained unknown how microtubule arrays are affected in *gem1* mutant microspores. Here, novel male gametophytic microtubule-reporter *Nicotiana tabacum* plants were constructed, expressing a green fluorescent protein-α-TUBULIN fusion protein (GFP-TUA6) under the control of a microspore-specific promoter. These plants allow effective visualization of all major male gametophytic microtubule arrays and provide useful tools to study the regulation of microtubule arrays by MAPs and other effectors. Depletion of *TMBP200*, a tobacco homologue of *MOR1/GEM1* in gametophytic microtubule-reporter plants using microspore-targeted RNA interference, induced defects in microspore polarity, division asymmetry and cytokinesis that were associated with striking defects in phragmoplast position, orientation, and structure. Our observations further reveal a requirement for *TMBP200* in gametophytic spindle organization and a novel role in spindle position and orientation in polarized microspores. These results provide direct evidence for the function of MAP215/Dis1 family protein TMBP200 in the organization of microtubule arrays critical for male germline formation in plants.

Key words: Asymmetric division, male germline, microspore, microtubule arrays, TMBP200 protein, tobacco pollen.

Introduction

For successful double fertilization during sexual reproduction in flowering plants, the male gametophyte provides two sperm cells that are produced from a distinct male germline after an elaborate developmental programme (McCormick, 2004; Borg *et al.*, 2009). Inside the anther locule, diploid microspore mother cells undergo meiosis to produce tetrads of haploid microspores encased in callose. After callose dissolution individual microspores undergo rapid cellular growth and polarization, involving migration of the nucleus to the future germ cell pole. The ontogeny of migration shows variation in different taxa, but the end-product is constant, a uninucleate polarized microspore (reviewed in Twell *et al.*, 1998). In *Arabidopsis* the centrally positioned microspore nucleus migrates to the pollen radial wall, while, in tobacco, the nucleus further translocates along the radial wall to one of the poles, where the microspore divides asymmetrically. As a result, the germline is established with the small germ cell isolated against the pollen wall. The germ cell is engulfed in the vegetative cell cytoplasm until it undergoes division to form the sperm cells. The control of germ cell cycle progression and gamete specification are under the control of a recently discovered E3 ubiquitin

ligase complex SCF^{FBL17} (Kim *et al.*, 2008; Gusti *et al.*, 2009) and the germline-specific MYB transcription factor DUO1 (Brownfield *et al.*, 2009), respectively. Although the control of microspore nuclear migration and division orientation are key processes in establishing the male germline, the cellular mechanisms involved remain poorly characterized.

Microtubules (MTs) are conserved in all eukaryotes and function during all types of cell division. In somatic plant cells, generally four alternating MT arrays are built regardless of division symmetry. During interphase, cortical MTs govern directional expansion for cell morphogenesis and three other successive MT arrays direct processes during cell division. The preprophase band (PPB) at G_2 phase marks the future division site, the spindle array segregates the duplicated chromosomes, and the phragmoplast array partitions the cytoplasm. There have been extensive investigations of dynamically alternating MT arrays with symmetrically dividing somatic cells and in asymmetrically dividing cells like meristemoid mother cells in the stomatal pathway (Wasteneys and Yang, 2004; Lucas *et al.*, 2006). On the other hand, MT arrays in male gametophyte development possess some unique features, such as the absence of the PPB to forecast the division plane and the assembly of an asymmetric spindle and a curved phragmoplast MT array (Terasaka and Niitsu, 1995; Zonia *et al.*, 1999). These gametophytic MT arrays have not been observed in live cells, representing a bottleneck for *in vivo* studies of the functional organization of gametophytic MTs and their regulators.

MAP215/Dis1 family proteins in eukaryotic taxa have crucial roles in cell division and morphogenesis through the regulation of MT stability and dynamics (Gard *et al.*, 2004). Founding members, XMAP215 and Dis1, were shown to promote MT assembly at the plus end in *Xenopus* eggs (Gard and Kirschner, 1987) and are essential for spindle function in yeast (Ohkura *et al.*, 1988). In *Arabidopsis gemini pollen 1* (*gem1*) mutants, microspores divide with incomplete asymmetry and often exhibit striking internal cell walls that arise from aberrant cytokinesis, in all cases failing to establish the germline (Park *et al.*, 1998; Park and Twell, 2001). The *gem1* phenotype was shown to arise from genetic lesions in the MAP215/Dis1 family gene *MICROTUBULE ORGANISATION1* (*MOR1*) (Whittington *et al.*, 2001; Twell *et al.*, 2002). MOR1/GEM1 co-localizes with all MT arrays during cell cycle progression in *Arabidopsis* cultured cells (Twell *et al.*, 2002) and in root cells (Kawamura *et al.*, 2006) and several independent studies have shown a requirement for MOR1/GEM1 in various microtubule arrays in somatic cells (Whittington *et al.*, 2001; Eleftheriou *et al.*, 2005; Kawamura *et al.*, 2006; Kawamura and Wasteneys, 2008). However, how the various MT arrays are affected in developing gametophytic cells that are deficient in MOR1/GEM1 remains to be investigated.

A role for MOR1/GEM1 in the MT arrays involved in nuclear migration and the phragmoplast was proposed based on aberrant microspore division phenotypes in *gem1* mutants (Twell *et al.*, 2002). However, the conserved role of MAP215/Dis1 proteins in spindle function in fungal and animal cells (Gard *et al.*, 2004) was not predicted for MOR1/GEM1 because nuclear division is always complete in *gem1* mutant spores (Park *et al.*, 1998). Similar predictions arose from the analysis of the allelic temperature-sensitive (ts) *mor1-1* and *mor1-2* mutants, as both were initially reported to disturb cortical MT arrays in root cells under restrictive conditions, but to show normal mitosis and cytokinesis (Whittington *et al.*, 2001). These results indicated that *mor1* and *gem1* might exhibit allele-specific defects on interphase cortical MT and phragmoplast MT arrays, respectively, but neither on the spindle. However, Eleftheriou *et al.* (2005) subsequently observed aberrant phragmoplasts in root cells of *mor1* mutants under more restrictive conditions and Kawamura *et al.* (2006) discovered mitotic defects arising from disordered spindles in *mor1* roots. These findings highlight the importance of experimental conditions and the analysis of multiple mutant alleles in different biological contexts to uncover the complete range of functions of MAP215/Dis1 proteins in plants.

Here, the gametophytic role of TMBP200, a tobacco orthologue of MOR1/GEM1 (Yasuhara *et al.*, 2002; Hamada *et al.*, 2004), and its requirement in the organization of the different MT arrays associated with asymmetric microspore division was investigated. To facilitate access to easily staged developing spores with substantially larger sizes and improved resolution of MT arrays, tools were developed for the analysis of native MT arrays and the functions of TMBP200 in tobacco microspores. A microspore-specific promoter was chosen to restrict both GFP-α-TUBULIN expression and TMBP200 RNA interference (RNAi) activity to male gametophytic cells. Combined analyses of DAPI staining of fixed spores and imaging of GFP-α-TUBULIN-decorated MT arrays demonstrate a requirement for TMBP200 in the organization of spindle and phragmoplast MT arrays associated with asymmetric mitosis. Our observations also reveal a novel requirement for TMBP200 in the control of spindle orientation required for germline establishment. The MT-reporter lines and targeted RNAi strategy developed in this study provide valuable tools for future detailed studies of the regulation and dynamic organization of MT arrays during male gametophyte development.

Materials and methods

Plant material and tobacco transformation

Nicotiana tabacum cv. SR1 wild-type and transgenic plants were grown under standard greenhouse conditions. For tobacco transformation, bleach-sterilized leaf discs from 6–8-week-old plants were co-cultivated with *Agrobacterium tumefaciens* GV3101 harbouring appropriate binary vectors. For antibiotic selection 75 mg l^{-1} kanamycin or 15 mg l^{-1} hygromycin were added to plant growth media. Plates were incubated at 25 °C under continuous fluorescent light. For RT-PCR analysis, mature pollen grains were harvested after brief vortex of open flowers in 0.3 M mannitol solution in 50 ml centrifuge tubes, filtration of the solution through 100 μm nylon mesh, and centrifugation at 3500 rpm for 15 min. Pollen pellets were flash-frozen in liquid nitrogen and stored at –80 °C until use.

Segregation analysis

Seeds from self-fertilized plants and from test crosses to wild-type plants were surface-sterilized with 100% ethanol for 2 min and germinated on plant growth media containing antibiotics.

RT-PCR analysis and vector constructions

Total RNA was extracted from approximately 100 mg of mature pollen using the RNeasy plant mini kit (Qiagen). First-strand cDNA was synthesized with 1 μg of total RNA and oligo-dT primers using the ImProm-II reverse transcription system (Promega) according to the manufacturer's instructions. PCR reactions were performed using 1 μl of the first-strand cDNA as a template and *TMBP200* gene-specific primers, which were also used for hp-TMBP200 RNAi vector construction as shown below. The *N. tabacum* actin gene was amplified as a constitutive control using primers: NtActinF, GATGCCTATGTTGGTGATGAAGCT and NtActinR, CACCATCACCAGAGTCCAACACAAT.

To target GFP-TUA6 expression to the microspore stage, the *NTM19* promoter sequence and GFP-TUA6 cassette were subcloned into pGreen0029 to create the ProNTM19:GFP-TUA6 vector that confers plant kanamycin selection. For tobacco hp-TMBP200 RNAi vector construction, cDNA fragments of ~500 bp were amplified by RT-PCR from 1 μg of total RNA extracted from *N. tabacum* cv. SR1 leaves using restriction enzyme site-tagged primers. After restriction enzyme digestion, DNA fragments were inserted downstream of the *NTM19* promoter cloned into an intermediate vector to create the TMBP200 inverted repeat, which was then transferred, together with the *NTM19* promoter, into a binary vector conferring hygromycin selection in plants. Primers used were as listed.

TGEMAHF, AAAAGTCGACGGCGCGCCAGTTCAGGAGAAGGCTCTTG

TGEMAHR, AAAAAAGCTTAGCAGTCCCCGTAACATTGAC

TGEMSEF, GGGGACTAGTTCAGGAGAAGGCTCTTGATGC

TGEMSER, GGGGGAATTCTTAGCAGTCCCCGTAACATTGAC

Microscopy

For histochemical analysis, fresh anthers and mature pollen were fixed in ethanol:acetic acid (3:1, v/v). DNA was stained with 0.8 μg ml^{-1} of 4,6-diamidino-2-phenylindole (DAPI) and callose walls with 0.1% aniline blue. Transmission electron microscopy was carried out as described previously (Park and Twell, 2001). For live spore imaging, spores freshly released from anthers or mature pollen were placed in 0.3 M mannitol solution and examined under bright field with DIC, under UV epifluorescence with a 41025 Piston GFP Bandpass filter set (Chroma Technology Corp. Bellows Falls, VT) or by confocal laser scanning microscopy on a Nikon T2000E inverted microscope with C1 confocal attachment (Nikon, Japan). Measurements of spindles and phragmoplasts were carried out using Open lab 4.4.4 (Improvision, Coventry, UK) and data were analysed for significant differences using a one-tailed *t* test (Excel software; Microsoft, Mountain View, CA). Images were processed with Adobe Photoshop CS2 (version 9.0).

Results

To investigate the role of TMBP200 in the diverse MT arrays associated with asymmetric microspore division, tobacco MT-reporter plants were generated that met three specific requirements: (i) that they express a MT-GFP marker protein during microspore division, (ii) are deficient in MAP215/Dis1 expression, and (iii) are free of developmental defects in vegetative or other reproductive cell types. This strategy required the tightly-regulated gametophyte-specific manipulation of plant MAP215/Dis1 expression, since plant MAP215/Dis1 is broadly expressed in somatic cells as well as gametophytic cells, rendering severe *mor1/gem1* alleles homozygous lethal. Therefore the tobacco microspore-specific *NTM19* gene promoter (Custers *et al.*, 1997) was used to induce the post-meiotic TMBP200 deficiency in microspores using a hairpin RNAi construct.

Generation of male gametophytic MT-GFP marker plants

The GFP-*Arabidiopsis*-α-tubulin 6 (GFP-TUA6) expression cassette was chosen as a proven MT-GFP marker. Cauliflower mosaic virus 35S promoter driven expression of GFP-TUA6, Pro35S:GFP-TUA6, is effective in visualizing MT arrays in somatic cells and in MT-defective mutant plants (Ueda *et al.*, 1999; Whittington *et al.*, 2001). However, use of the CaMV 35S promoter to drive GFP-TUA6 expression may not be optimal because Pro35S:GFP-TUA6 plants exhibit right-handed helical growth and left-handed helical MT array organization in aerial tissues where the expression level is much higher (Abe and Hashimoto, 2005). Thus, the microspore-specific *NTM19* promoter was used to confine GFP-TUA6 expression to male gametophytic cells and to minimize potential non-target effects of modified TUA6 expression on MT organization during vegetative growth.

Twenty-one independent *Nicotiana tabacum* cv. SR1 plants containing the ProNTM19:GFP-TUA6 marker were generated. All lines showed normal vegetative growth, leaf and flower morphology and 19 lines had detectable GFP in mature pollen. Four single locus lines that segregated approximately 50% GFP-positive pollen with low, intermediate or high levels of GFP expression were characterized. Self progeny analysed for three of these lines showed the expected ~3:1 ratio of kanamycin-resistant to -sensitive progeny (data not shown), indicating that GFP-TUA6 expressing pollen competes equally with wild-type pollen, and does not cause genetic abnormalities. Further examination of developing spores showed that MT arrays in microspores and germ cells were clearly and consistently labelled in all four lines (detailed below).

ProNTM19:GFP-TUA6 marker plants display normal pollen development

DAPI staining of developing spores in the four selected ProNTM19:GFP-TUA6 lines verified that pollen development was normal (Fig. 1). A standard format was adopted for the orientation of images of spores, that is indicated in the text and on images where relevant (see diagrams inserted in Figs 1, 2 and 4, 5 for reference). Radial view shows pollen with the polar axis from top to bottom, pollen apertures not visible. Germ pole view (GP) represents a transverse plane through the polar axis at the germ cell pole with the apertures evenly spaced in the pollen outer wall (exine).

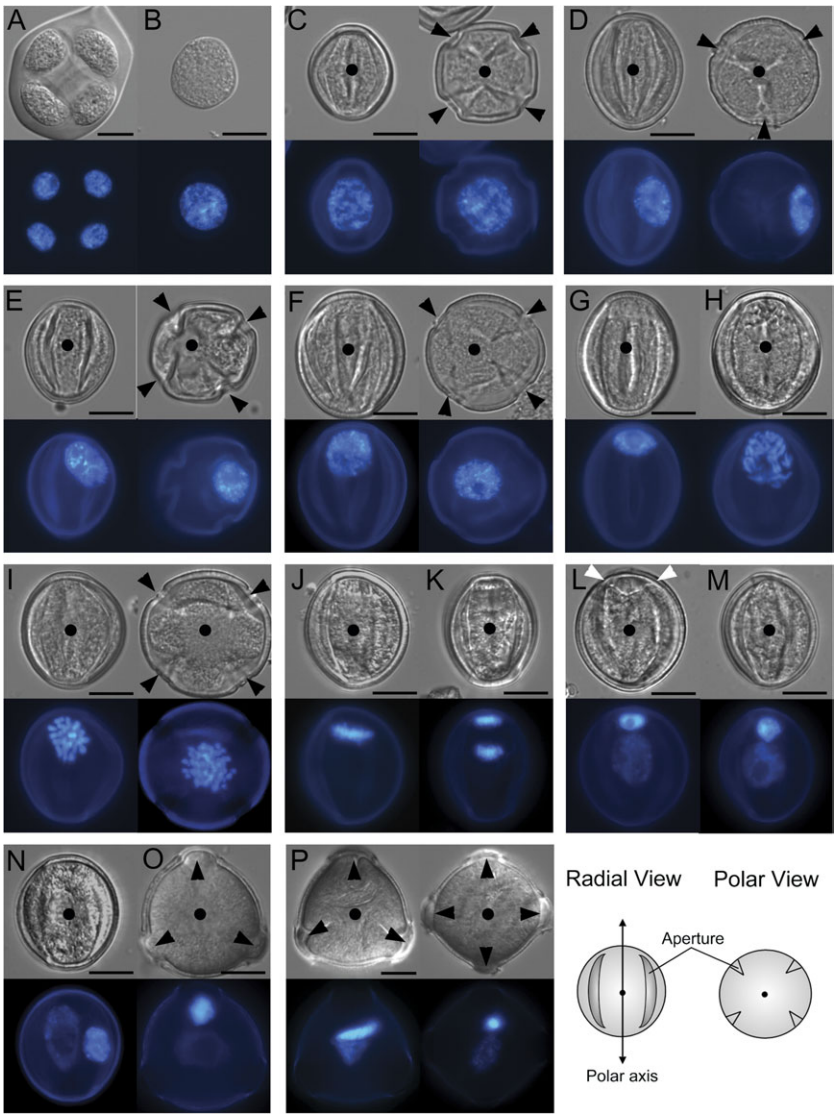

Fig. 1. Pollen development in ProNTM19-GFP::TUA6 transgenic plants. DAPI-stained spores/pollen are viewed with DIC (upper panel) or in epifluorescence (lower panel) from tetrad (A), early microspore just after callose dissolution (B), microspore before nuclear migration (C), after the first equatorial nuclear migration (D), during (E) and after the second polar migration (F, G), during (H–K) and after microspore division (L–O), and mature pollen (P) stages. Images left or right represent views from the radial wall or germ cell pole (GP) (C–F, I). Black arrowheads indicate apertures and filled circles are equivalent to marks on the diagram as an orientation reference. White arrows indicate the germ cell wall attached to the pollen wall. Size bars depict 10 μm.

Normal development observed in wild-type and marker plants is shown in Fig. 1. A tetrad of four haploid microspores (Fig. 1A) and free microspores after callose dissolution (Fig. 1B) indicate normal meiosis and microspore production. Early microspores with a central nucleus possess three or four apertures (Fig. 1C, radial and GP views). In later microspores, the nucleus migrates first to the radial wall at the equator (Fig. 1D, radial and GP views) and then along the radial wall (Fig. 1E, radial and GP views) to the future GP (Fig. 1F, radial and GP views). Before entering mitosis the microspore nucleus is flattened against the GP (Fig. 1G, radial view). Figures 1H–K show prophase to anaphase during mitosis. Metaphase chromosomes always align perpendicular to the polar axis (n=62, Fig. 1J, radial view) and two sets of anaphase chromosomes separate along the polar axis (Fig. 1K, radial view), resulting in two daughter nuclei with distinct DAPI-staining intensity and size (Fig. 1L, radial view). At the early bicellular stage, a curved cell wall separates the smaller germ cell with an intensely DAPI-stained nucleus at the GP from the larger vegetative cell with a more diffuse DAPI-staining nucleus (white arrows in Fig. 1L). At the mid-bicellular stage, the germ cell and vegetative nucleus migrate inwards (Fig. 1M, radial view; Fig. 1N, O, radial and GP views). The germ cell nucleus subsequently undergoes morphogenesis to a highly elongated cigar-shape in mature pollen (Fig. 1P). The absence of abnormal nuclear and cell division events in ProNTM19:GFP-TUA6 pollen and its normal genetic segregation compared with wild-type pollen indicates authentic function of associated MT arrays during

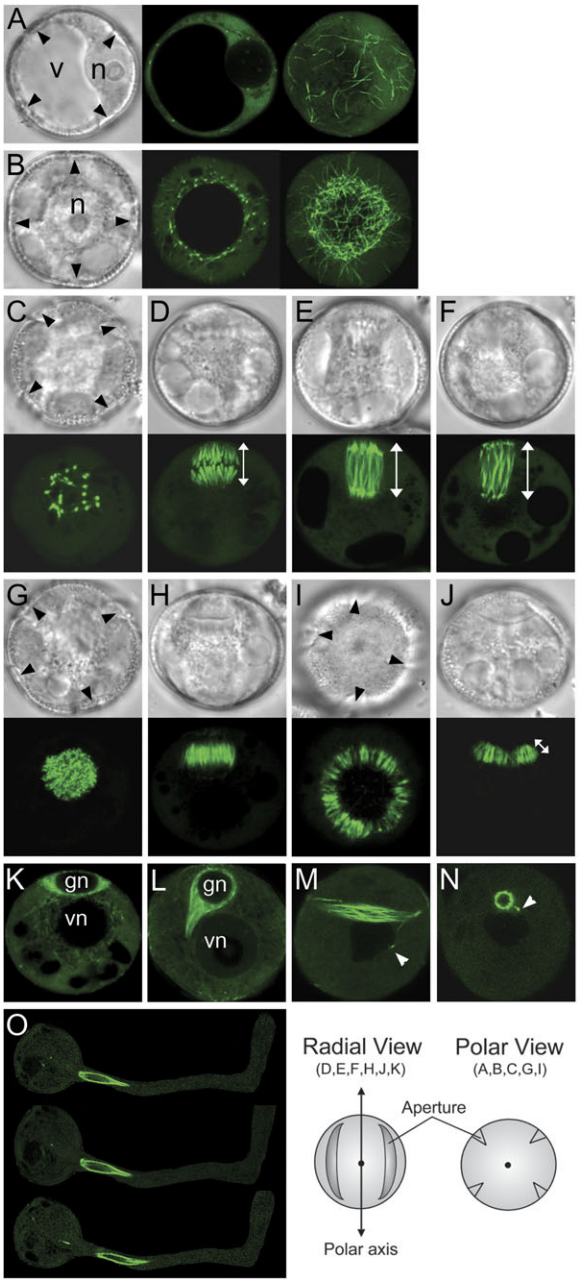

Fig. 2. Live spores and pollen from ProNTM19-GFP::TUA6 transgenic line. Fresh spores and pollen viewed with DIC (grey) or with CLSM (green). (A, B) polarizing microspores, (C–J) microspores during mitosis, (K) early and (L) mid-bicellular pollen, (M, N) mature pollen. Microspores after equatorial nuclear migration (A) and after polar nuclear migration (B). Microspores are viewed as a single optical section (centre) or as projections of z-series (right) from the GP. (C–F) Microspores undergoing nuclear division are viewed from the GP (C) or from the radial wall (D–F). Mitotic spindles at metaphase (D), anaphase (E), and telophase (F). Images are single optical sections (C, E, F) or a projection of a z-series (D). (G–J) Microspores undergoing cytokinesis are viewed from the GP (G, I) or from radial wall (H, J). The phragmoplasts at early (G, H) or at later (I, J) stages. Images are single optical sections. (K–O) Fresh spores after microspore mitosis and mature pollen freshly dehisced or incubated in germination media are viewed. Early bicellular (K), mid-bicellular spores (L), mature pollen (M, N) or germinated pollen at three successive minute intervals, top to bottom (O). Images are single optical sections. Black arrowheads indicate apertures seen from the future GP. White arrowheads indicate a MT-rich tail connecting the germ cell and vegetative nucleus. v, Microspore vacuole; n, microspore nucleus; gn, germ cell nucleus; vn, vegetative nucleus. An orientation schematic for the images is shown. The white line with double arrow heads represents length measured for metaphase (D) and anaphase to telophase (E, F) spindles and for the phragmoplast (J).

male gametophyte development. Hereafter, our detailed analysis of MT organization was focused on one homozygous line (C5) with intermediate GFP-TUA6 expression.

Visualization of in vivo *MT arrays with unique features in microspore and developing pollen*

MT arrays labelled with GFP-TUA6 were monitored during microspore and pollen development. GFP expression driven by the *NTM19* promoter is not detectable in early microspores but becomes prominent during the course of nuclear migration (Fig. 2A, B). When the microspore nucleus had moved to the radial wall, GFP signals were first observed as a limited number of bright spots around the nucleus and the single large vacuolar envelope, as well as in cortical MTs (Fig. 2A, GP view) that gradually increased in number and brightness. When the microspore nucleus was positioned near the germ cell pole, a dense network of perinuclear MTs extends towards the cortex (Fig. 2B, GP view). This 'woven ball- or basket-like' structure forms a cortical cap of MTs at the GP closely associated with the nuclear envelope. This MT array may help to direct or maintain an eccentric nuclear position prior to asymmetric division.

As each microspore enters mitosis, interphase MT arrays are reorganized into the mitotic spindle. Figure 2C–F show the typical form and orientation of the spindle. The spindle viewed from the GP is always observed as a group of thick spots that reflects a broad GP half spindle (Fig. 2C, GP view). Thus, spindle polarity and form is tightly controlled. Previous studies using immunostaining of MTs showed asymmetric spindles in microspores from *Tradescantia* (Terasaka and Nittsu, 1995) and tobacco (Zonia *et al.*, 1999). Consistent with these results, asymmetric spindles were observed in live tobacco microspores of which the GP half spindle is broader and less focused than the vegetative cell pole half spindle (Fig. 2D–F, radial views). Metaphase chromosome-capturing spindle MTs showed relatively uniform GFP signals along their length (Fig. 2D). During anaphase GFP signals were stronger at the ends of the spindle than in the interzone (Fig. 2E), but became more equal along the highly extended spindle at late anaphase (Fig. 2F).

Upon completion of chromosome separation, densely packed MTs in the midzone of the telophase spindle initiate the phragmoplast. The phragmoplast initial appears as a compact round plate filled with fine MTs (Fig. 2G, GP view) and as a short twin comb-like array (Fig. 2H, radial

view). To guide the hemispherical cell plate enclosing the germ cell, the phragmoplast expands as a specialized double ring structure, with a smaller ring of MTs closer to the GP, which is maintained during centrifugal growth (Fig. 2I, J, GP and radial views).

Further changes in MT arrays were also observed after asymmetric microspore division (Fig. 2K–O). GFP signals were stronger in the newly formed germ cell than in the vegetative cell cytoplasm (Fig. 2K), which probably reflects the equal segregation of free GFP-TUA6 dissociated from phragmoplast MTs, but in unequal cytoplasmic volumes. Localized GFP signals in the vegetative cell at this stage indicate perinuclear bundles of MTs that are absent at later stages. After the nascent germ cell is engulfed, germ cell MTs gradually assemble into thick axially aligned cortical MT bundles, which represents a cortical MT array implicated in germ cell morphogenesis (Fig. 2L–N; Sanger and Jackson, 1971; Tanaka *et al.*, 1989; Theunis *et al.*, 1992). Figure 2M–O show the physical connection of the germ cell to the vegetative cell nucleus by a MT-rich cytoplasmic tail that is maintained in germinating pollen grown *in vitro* (Fig. 2O). In summary, cortical, spindle, and phragmoplast MT arrays were visualized in polarizing microspores and developing pollen expressing the ProNTM19:GFP-TUA6 marker.

TMBP200 RNAi induces gem1*-like and unique pollen phenotypes*

To investigate the role of TMBP200 in gametophytic MT organization, an RNAi vector (ProNTM19-hp-TMBP200) was constructed and stably introduced into MT-reporter line C5, homozygous for ProNTM19:GFP-TUA6. Eighteen T_1 plants were obtained and screened for pollen phenotypes. At the mature pollen stage all TMBP200 RNAi lines produced mutant phenotypes characteristic of *Arabidopsis gem1* pollen, including equally divided bicellular, binucleate, uninucleate, and aborted pollen (Park *et al.*, 1998; Park and Twell, 2001; Twell *et al.*, 2002). Independent transformants showed weak, intermediate or severe phenotypes, with weak lines showing less than 10% aberrant pollen and severe lines over 50%, with a high proportion of aborted pollen. Examination of early bicellular stage pollen in multiple lines from all three groups showed consistent phenotypes that are described below.

In wild-type early bicellular pollen, the division plane is always aligned perpendicular to the pollen polar axis isolating the germ cell at the GP (Fig. 3A, radial view). By contrast, early bicellular pollen from TMBP200 RNAi plants displayed a range of division planes with altered angles and complex wall profiles (Fig. 3B–H, radial views). Pollen exhibiting altered division planes (Fig. 3B–E) indicates that division occurs after incomplete nuclear migration and results from altered spindle and phragmoplast orientations. Interestingly, three unequal nuclei (Fig. 3H) instead of two were often observed, which could result from abnormal chromosome segregation arising from spindle defects.

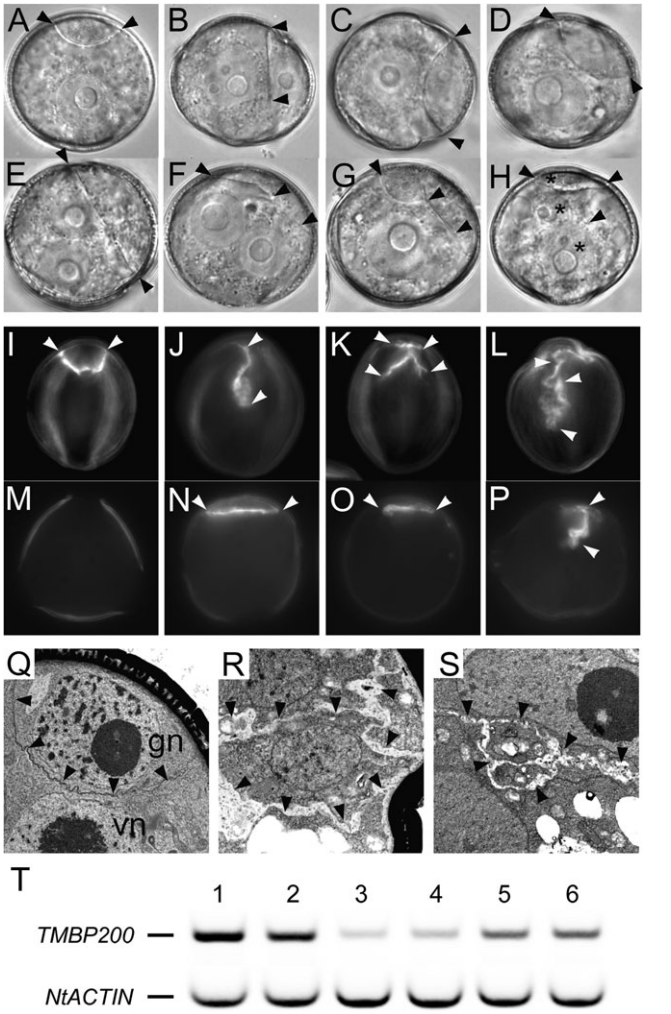

Fig. 3. Verification of the link between mutant phenotype and *TMBP200* expression in TMBP200 RNAi plants. (A–H) Fresh spores from wild type (A) or RNAi lines (B–H) are viewed with DIC. Black arrowheads indicate the position of walls. Three arrowheads (F–H) indicate the complex profile of walls and asterisks (H) indicate three nuclei. (I–P) Callose staining of walls with aniline blue. White arrowheads indicate aniline blue stained walls. Fixed spores at early bicellular (I–L) and mature pollen (M–P) stages viewed by epifluorescence. In contrast to wild-type pollen (I, M) showing a lens-shaped callose wall only at the early bicellular stage, mutant pollen from RNAi lines display complex and persistent callose walls (J–L, N–P). (Q–S) Transmission electron micrographs of pollen at the bicellular stage. While wild-type pollen shows a smooth and hemispherical barrier between the two daughter nuclei (Q), mutant pollen displays highly complex walls (R, S) similar to those observed in *gem1*. Black arrowheads outline the walls. (T) RT-PCR analysis using mature pollen RNA and *TMBP200*-specific primers. A tobacco actin gene, *NtACTIN*, was used as the internal control to show an equivalent amount of cDNA templates were used between samples. C5 control plants (lanes 1, 2) and two intermediate TMBP200 RNAi plants, line 18 (lanes 3, 4) and line 20 (lanes 5, 6), were analysed in duplicate from separately prepared RNA samples.

The complex cell wall profiles observed in some pollen (Fig. 3F–H) suggest disorganized phragmoplasts, which have been observed in *mor1* roots incubated at restrictive temperatures (Eleftheriou *et al.*, 2005; Kawamura *et al.*, 2006). Internal wall profiles were examined in fixed spores from TMBP200 plants. Figure 3I–P show callose walls stained with aniline blue at the early bicellular and mature pollen stages. In wild-type pollen, aniline blue stains the hemispherical callose wall where the germ cell remains attached to the pollen wall but not at later stages (Fig. 3I, M). (Note that non-callosic autofluorescence of the exine wall layer is also observed at the UV wavelengths used to visualize aniline blue staining). By contrast, callose staining in abnormal spores from TMBP200 RNAi plants is highly irregular at the early bicellular stage (Fig. 3J–L) and persists with less complexity until the mature pollen stage (Fig. 3N–P), as in *gem1* pollen (Park and Twell, 2001). Examination of the ultrastructure of abnormal bicellular pollen grains in TMBP200 RNAi plants by transmission electron microscopy (Fig. 3Q–S) further confirmed the presence of complex wall profiles with excessive callose deposition.

Genetic analysis of TMBP200 RNAi plants confirmed that the presence of ProNTM19-hp-TMBP200 conferred male gametophyte-specific phenotypes. Selfed progeny from single locus TMBP200 RNAi lines showed reduced inheritance of ProNTM19-hp-TMBP200, with distorted segregation ratios of 1.3–1.7:1 rather than the expected 3:1 ratio indicating gametophytic transmission defects (Table 1). The genetic transmission efficiency (TE) of ProNTM19-hp-TMBP200 was found to be severely inhibited through the male (TE ~25%). Transmission was normal through the female (TE ~100%) resulting in a 1:1 ratio of wild-type and hemizygous TMBP200 RNAi plants with pollen defects. Thus, the *NTM19* promoter directs male gametophyte-specific defects in tobacco plants that are stably propagated through the female.

In order to verify the predicted knockdown of *TMBP200* expression in RNAi plants, semi-quantitative RT-PCR was carried out using RNA isolated from mature pollen. Figure 3T shows a significant reduction of *TMBP200* transcripts in pollen of TMBP200 RNAi lines (lanes 3–6) compared to WT control plants (lanes 1–2), demonstrating the link between *gem1*-like phenotypes and TMBP200 down-regulation.

Table 1. Genetic transmission of ProNTM19-hp-TMBP200

Two independently transformed hemizygous lines used contain a single locus ProNTM19-hp-TMBP200 transgene. Seeds were harvested after self or reciprocal crosses to wild-type plants. Seedlings were grown on plates containing MS plant media supplemented with 15 mg l^{-1} hygromycin and the resistant (R) and sensitive (S) seedlings were scored.

Line	Self		Male		Female	
	R/S	Ratio	R/S	Ratio	R/S	Ratio
TMBP200RNAi-5	84/49	1.7:1	17/61	0.28:1	63/56	1.13:1
TMBP200RNAi-7	81/61	1.3:1	26/106	0.25:1	54/53	1.02:1

Impaired microspore polarity and mitosis in TMBP200 RNAi lines

Figure 4 depicts mutant phenotypes in developing spores of TMBP200 RNAi lines after DAPI staining. Early microspore development in the RNAi lines is indistinguishable from the wild type, but a proportion of dividing microspores show mitotic figures in abnormal locations as a clear demonstration of incomplete nuclear migration (Table 2; Fig. 4A–D, radial views). For instance the abnormal onset of mitosis in unpolarized microspores (Fig. 4A) indicating complete failure or unstable nuclear migration, that is not detected in control plants, was typically observed in 2–5% of microspores in TMBP200 RNAi lines (Table 2). There is also indirect but strong evidence for spindle defects that includes lagging chromosomes (Fig. 4E–H, radial views), tilted alignments and separation of duplicated chromosomes that are often perpendicular to or oblique to the normal spindle orientation (Fig. 4H–K, radial views), and extra groups of anaphase chromosomes (Fig. 4L, radial view). The frequency of microspores undergoing abnormal meta-ana-telophases was observed to be 8.1% in a TMBP200 RNAi line (Table 2). Abnormal phenotypes just after microspore division include spores with two daughter nuclei nearly identical in size, either displaced towards the GP or more centrally located (Fig. 4M–N, radial views), and the formation of micronuclei (Fig. 4O, P, radial views) at a frequency of 13% and 17.3%, respectively (Table 2). The occurrence of novel phenotypes indicating spindles with altered orientation, but normally positioned at the GP, distinguishes two steps in polar cell division, nuclear migration and spindle orientation. Thus, even when nuclear migration appears normal, spindle orientation can be impaired in TMBP200-deficient microspores (Fig. 4I, M). At the mature pollen stages, the majority of abnormal pollen phenotypes are binucleate (Fig. 4Q), uninucleate arising from nuclear fusion (Fig. 4R), or aborted pollen (Fig. 4S).

Visualization of aberrant MT arrays in TMBP200 RNAi lines

Abnormal spores with micronuclei (Fig. 4O, P) and complex wall profiles (Fig. 3) indicate disruption of spindles and phragmoplasts in TMBP200-deficient microspores. By imaging MTs decorated by GFP-TUA6, a marked range of such disruptions *in vivo* was confirmed. In wild-type microspores, a bipolar spindle was established at the GP with the spindle axis always aligned with the pollen polar axis. When observed from the GP, the broad end of the GP half spindle can be seen [Figs 2C, 5; Wt Spi (P)] and in radial view the entire spindle structure [Figs 2D–F, 5; Wt Spi (R)]. By contrast, microspores from TMBP200 RNAi plants showed disruption of both spindle structure and orientation. Bipolar spindles were often formed but at tilted angles (Fig. 5A–C). Figure 5A shows an abnormal spindle at metaphase viewed from the radial wall, which is bipolar but perpendicular to the normal spindle orientation (Fig. 5 Wt Spi (R), and Fig. 2D). Figure 5B and C show abnormal

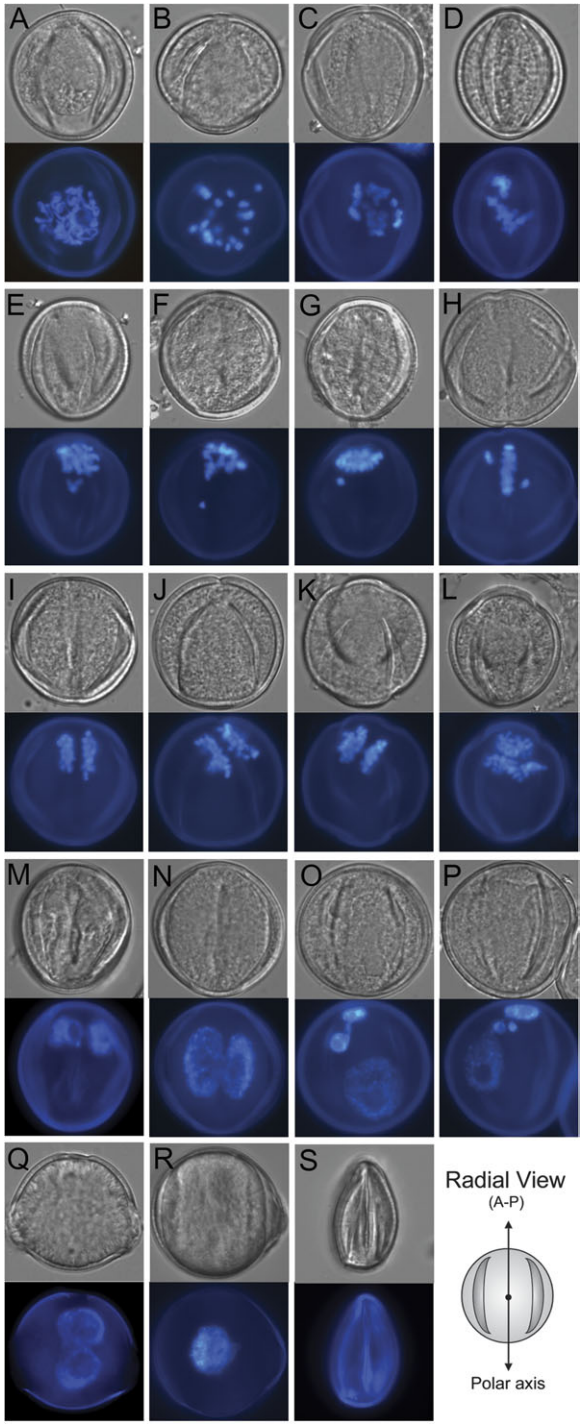

Fig. 4. Pollen development in TMBP200 RNAi lines. Fixed spores were stained with DAPI and viewed by DIC (upper panels) or epifluorescence (lower panels). Microspores undergoing mitosis with impaired polarity (A–D), microspore showing lagging chromosomes (E–H) or misaligned chromosomes at meta-anaphase (H–L), pollen after mitosis showing two equal nuclei at the pole (M) or in the centre (N) or micronuclei (O, P) at the bicellular stage, binucleate (Q), fusion nucleate (R) or aborted pollen (S) at the mature pollen stage. Images are shown in a radial view (A–P) except for those at the mature pollen stage (Q–S). An orientation schematic for the images is shown.

bipolar spindles at ana/telophase, which are rotated by 90° causing both ends of the spindle to be exposed to the GP. This structure appears similar to wild-type spindles viewed from the radial wall (Fig. 2E, F), but much shorter in length (see below for details). Spindle bipolarity is also severely disrupted in many cases. Multi-polar spindles with half spindles often of different length were observed (Fig. 5D–F), which are typically seen in cells lacking the *Drosophila* XMAP215/Dis1 orthologue Mini spindles (Gard *et al.*, 2004). These multipolar spindles are the probable cause of the unequal mitotic segregation and micronuclei phenotypes observed in TMBP200 RNAi lines (Fig. 4O, P).

At later stages, abnormal spores proceed into cytokinesis with disoriented or disorganized phragmoplasts. Multiple examples that typically fall into two classes are shown in Fig. 5G–L. Single continuous phragmoplasts but with abnormal position, profiles, or orientation (Fig. 5G, H) are likely to be initiated from misoriented bipolar spindles. Complex, branched or fragmented phragmoplasts (Fig. 5I–L) are also attributed to multipolar spindles. In turn, these complex phragmoplast forms account for the synthesis of the striking profiles of internal cell walls observed in TMBP200 RNAi lines.

Previous reports have described the reduced length of spindles of phragmoplasts in *mor1* roots under restrictive temperatures (Kawamura *et al.*, 2006). Spindle and phragmoplast lengths, visualized by GFP-TUA6, were also measured in microspores from wild-type and TMBP200 RNAi plants at equivalent stages (Table 3). Measurement of comparable dimensions marked in Fig. 2D or Fig. 2E and F for spindles at metaphase or ana/telophase respectively, and Fig. 2J for expanding phragmoplasts, revealed that spindles at two typical mitotic stages and phragmoplasts are both significantly shorter in microspores from TMBP200 RNAi plants. This indicates that *TMBP200* has a role in spindle and phragmoplast morphology in tobacco gametophytic cells, similar to that demonstrated for MOR1/GEM1 in sporophytic cells in *Arabidopsis* (Kawamura *et al.*, 2006).

Discussion

In this study the gametophytic requirement for plant MAP215/Dis1 protein function during tobacco male germline establishment was investigated. Gametophytic MT arrays were visualized from late microspore to mature pollen stages using gametophytic MT-GFP-reporter plants generated in this study. Then a microspore-targeted RNAi approach that knocked down *TMBP200* expression revealed a requirement for *TMBP200* in three successive steps during asymmetric division, nuclear positioning during interphase, mitosis and cytokinesis. These findings further demonstrate an important role for TMBP200 in spindle and phragmoplast MT organization during male germline establishment in tobacco.

Novel male gametophytic MT-marker plants in tobacco

In previous work Zonia *et al.* (1999) provided pharmacological evidence that unique MT arrays function during

Table 2. Phenotypic classification of DAPI-stained spores in control and TMBP200 RNAi lines

DAPI-stained spores were counted using single anther samples in control ProNTM19:GFP-TUA6 line C5 and TMBP200 RNAi line 23 at three successive developmental stages. Frequencies of total aberrant spores and each aberrant type are shown. Note that a proportion of abnormal spores classified into abnormal meta-ana-telo phases and two equal nuclei in the RNAi line might arise from microspores classed as unpolarized onset of mitosis.

		Control ProNTM19:GFP-TUA6			TMBP200 RNAi		
		C5	C5	C5	Line 23	Line 23	Line 23
Normal class	Early microspore	493	34		264	12	
	Polarizing mid-late microspore		475	41	9	177	34
	Polarized onset of mitosis			38			92
	Meta-ana-telophases			32			31
	Early bicellular			253			153
	Mid-bicellular			1			10
Abnormal class	Unpolarized onset of mitosis			0 (0%)			22 (4%)
	Abnormal meta-ana-telophases			0 (0%)			45 (8.1%)
	Two equal nuclei			0 (0%)			72 (13%)
	Micro nuclei			0 (0%)			96 (17.3%)
Spores counted (% of aberrant spores)		493 (0%)	509 (0%)	354 (0%)	273 (0%)	189 (0%)	555 (42.3%)

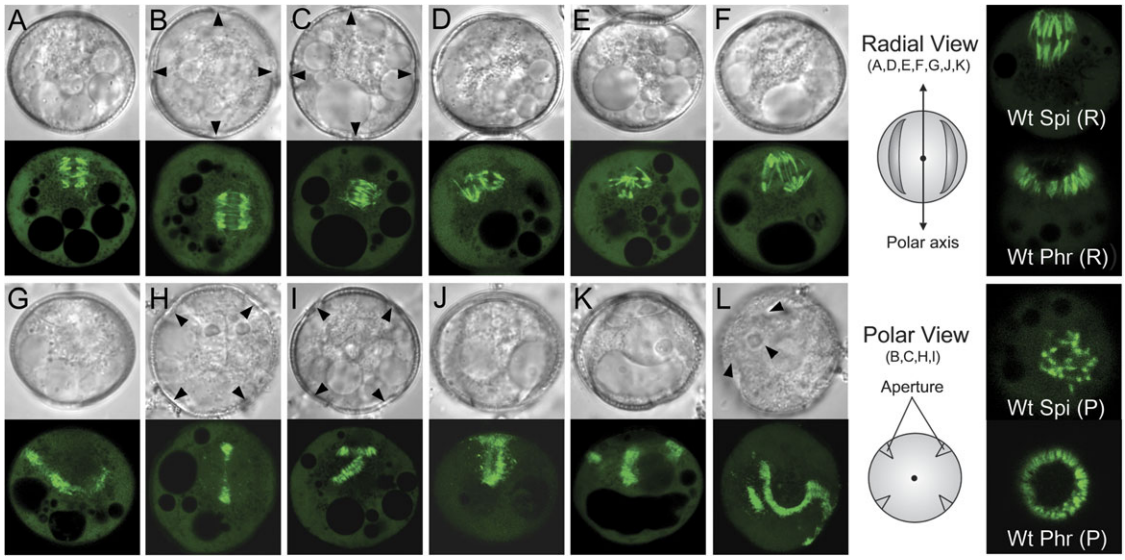

Fig. 5. Mitotic and cytokinetic apparatus in TMBP200 RNAi lines. Spindles (A–F) and phragmoplasts (G–L) from microspores undergoing aberrant mitosis or cytokinesis were viewed with DIC (upper panel) and with CLSM (lower panel). Images are shown in radial view (A, D, E, F, G, J, K), GP view (B, C, H, I) or at an angle in between (L). Arrowheads (B, C, H, I, L) indicate positions of pollen apertures. Mutant spindles represent bipolar spindles 90° rotated (A, B, C) and multipolar spindles (D, E, F). Mutant phragmoplasts represent single but misoriented (G, H) and complex branched or fragmented forms (I, J, K, L). An orientation schematic and wild-type spindle and phragmoplast images are shown for radial (R) and polar (P) views.

microspore development in tobacco by immunostaining with β-tubulin antibody. Here MT arrays with GFP-TUA6 incorporated were visualized in live microspores and pollen in stable male gametophytic MT-reporter plants. Tubulin-protein reporters for MTs are known to label MT arrays uniformly along the length, but there has been some concern related to the overexpression of modified tubulins (Ueda *et al.*, 1999; Wasteneys and Yang, 2004; Abe and Hashimoto, 2005; Burk *et al.*, 2006). Bearing this in mind, GFP-TUA6 expression was restricted to microspores and a line with medium expression of GFP-TUA6 was selected allowing us to detail MT arrays in male gametophytic cells without causing aberrant gametophyte development or ectopic plant growth defects.

Using live spores, the ProNTM19:GFP-TUA6 marker successfully revealed various cell cycle-specific MT arrays that exhibit characteristics consistent with previous reports on immunolocalized MT arrays in male gametophytic cells. Prior to microspore division, interphase cortical and perinuclear MTs were organized concurrently with nuclear

Table 3. Measurements of spindle and phragmoplast length in wild-type and TMBP200 RNAi lines

Spindle and phragmoplast lengths were measured in microspores of three independent RNAi lines and the mean values of pooled data are shown. *T* test values were calculated using a one-tailed *t* test (Excel software; Microsoft, Mountain View, CA).

	Metaphase spindle	Ana/telophase spindle	Phragmoplast
Wild type	7.98±0.86 (n=44)	11.26±1.33 (n=21)	3.32±0.33 (n=61)
TMBP200 RNAi	5.42±0.84 (n=52)	8.36±1.08 (n=6)	2.43±0.38 (n=50)
t test	2.21×10^{-26}	6.77×10^{-5}	5.26×10^{-17}

migration. With immunostaining, Zonia *et al.* (1999) reported the presence of a MT 'basket' structure enclosing the premitotic microspore nucleus in tobacco. Our findings reveal the native organization of this unique GP basket-like MT array or nuclear cap that is associated with the polarization of the microspore prior to asymmetric division.

In order to achieve the correct division plane, plant cells decipher positional cues between the nucleus and cell cortex as in other eukaryotic cells (Muller *et al.*, 2009). In somatic plant cells, the temporary PPB band encircling the nucleus marks the future division plane and the position of the PPB has been shown to be influenced by the nucleus, although not exclusively (Muller *et al.*, 2009). The PPB plays a role in spindle assembly and orientation and, in turn, the spindle facilitates phragmoplast orientation (Muller *et al.*, 2009). Therefore nuclear position and the PPB significantly influence the cell division plane in somatic cells. The MT-dependent migration of the microspore nucleus in different species (Terasaka and Niitsu, 1987; Eady *et al.*, 1995) and division without the PPB highlights the role of other premitotic MT structures in the position and orientation of the division plane. It is possible that the GP basket-like nuclear cap of MTs, that connects the nuclear envelope and cortex, functions to stabilize nuclear position at the GP in tobacco microspores. The nuclear surface is a prominent MT nucleation site in plants and might play a more prominent role in polarized microspore division, including specification of the division plane, than in other types of division using the PPB.

In mitotic microspores expressing the GFP-TUA6 reporter, the bipolar spindle with a fixed orientation and an asymmetric form completed typical morphological changes. During cytokinesis the MTs of the phragmoplast initial formed a typical double ring structure that was organized from the spindle mid-zone and centrifugally displaced to the leading edge of the nascent cell plate, thus maintaining the smaller ring towards the GP as a result of the unequal expansion of phragmoplast MTs on either side of the cell plate. Secondly, after microspore division, initial engulfment and rounding up of the germ cell, cytoplasmic MTs in the germ cell are gradually bundled into cortical MTs associated with germ cell morphogenesis to form a cigar-shape. Germ cell elongation is widely conserved and may be adopted to facilitate its association with the vegetative cell nucleus to form the male germ unit (MGU) and/or its intracellular transport through the narrow pollen tube (Dumas *et al.*, 1998; Lalanne and Twell, 2002). The germ cell was observed to be connected to the vegetative cell nucleus with a MT-rich cytoplasmic tail to form the male germ unit (MGU). The MGU that is thought to aid co-ordinated delivery of the gametes was observed to be maintained in pollen tubes during *in vitro* pollen germination (Fig. 2O). These observations and the applications discussed below demonstrate the value of ProNTM19:GFP-TUA6 lines to monitor MT arrays during asymmetric microspore division and male germ cell development in tobacco.

Microspore-targeted RNAi reveals TMBP200 loss-of-function effects

Transgenic tobacco microspores expressing GFP-α-TUBULIN in conjunction with the hp-TMBP200 RNAi construct revealed phenotypes similar to *gem1* loss-of-function mutants, indicating that plant MAP215/Dis1 homologues have conserved functions in pollen development. Moreover, the marked range of disordered phragmoplasts induced in *TMBP200*-depleted microspores demonstrates its requirement for the organization of phragmoplast MTs in tobacco that is consistent with predicted functions for MOR1/GEM1 in *Arabidopsis* microspores (Twell *et al.*, 2002).

Striking mitotic defects that had not been detected in *Arabidopsis gem1* mutants were observed in tobacco TMBP200 RNAi lines. The lack of mitotic defects in *Arabidopsis gem1* mutants may be explained by the inheritance of sufficient MOR1/GEM1 through meiosis in *gem1* heterozygotes to mask its role in the spindle, or there may be a reduced gametophytic requirement for MOR1/GEM1 in *Arabidopsis* spindles. Our results extend the conserved role of MAP215/Dis1 family proteins in mitotic spindle organization to male gametophytic cells. Tobacco microspores might therefore offer a better environment to reveal hidden defects by virtue of the greater size and complexity of the mitotic spindle required to segregate a significantly larger number of chromosomes in tobacco ($2n$=42) than in *Arabidopsis* ($2n$=10).

Our results also clearly reveal a requirement for *TMBP200* in nuclear positioning prior to asymmetric microspore mitosis. A role for MOR1/GEM1 in nuclear migration was suggested, based on the analysis of *Arabidopsis gem1* mutants (Park *et al.*, 1998), but a novel requirement for TMBP200 in the normally tight control of microspore spindle orientation was revealed in this study. Since *Arabidopsis gem1* mutant microspores appear to undergo relatively normal division planes it had not been suspected that plant XMAP215/Dis1 proteins might be important in the control of spindle orientation (Park *et al.*,

1998). However depletion of *TMBP200* caused random spindle orientation and division planes in both polarized and unpolarized microspores. This suggests that division plane control may be linked to taxa-specific nuclear migration and that spindle orientation in polarized tobacco microspores is not simply determined by nuclear position. Our observations distinguish two steps in the control of division asymmetry in tobacco microspores that depend on TMBP200, nuclear positioning at the GP and determination of the spindle axis. Furthermore, when combined with future practical improvements in *in vitro* microspore culture and single cell imaging, the lines generated in this study will be useful to investigate the *in vivo* dynamics of MT arrays unique to the male gametophyte in depth, as well as MT structures affected by different chemical or biological effectors. This will enable comparative studies of the roles of various MAPs in both somatic and male gametophytic cells that possess cell type-specific differences in MT arrays.

Functional role of plant MAP215/Dis1 family proteins MOR1/GEM1 and TMBP200

Insights into the mechanisms by which the MAP215/Dis1 family proteins exert their functions in MT dynamics have been gained from different systems. Yasuhara *et al.* (2002) isolated TMBP200 from telophase tobacco BY-2 cells and reported its MT bundling activity that cross-bridges MTs into bundles in a distance comparable to those observed in phragmoplasts in *Haemanthus* and tobacco BY-2 cells, suggesting that TMBP200 may participate in the formation of MT bundles in phragmoplasts. On the contrary, TMBP200/MAP200, purified from interphase-enriched tobacco BY-2 cells did not show MT bundling activity (Hamada *et al.*, 2004). Instead, MAP200 increased both the length and number of MTs in a concentration-dependent manner and bound tubulin dimers, suggesting that MAP200 may be a molecular shuttle to supply tubulin dimers to the MT plus end.

In Arabidopsis, Kawamura *et al.* (2006) showed that spindles and phragmoplasts in *mor1* root cells are significantly shorter at restrictive conditions. TMBP200 RNAi microspores also displayed shorter spindles and phragmoplasts. This tendency is in accord with the results of recent *in vitro* experiments showing that *Xenopus* MAP215 accelerates tip growth at the plus end of MTs as a processive polymerase depending on concentration (Brouhard *et al.*, 2008). Shorter spindles, often with multipolarity in TMBP200 RNAi lines, indicates a failure to stabilize the growth of two opposing poles of MTs and to suppress other sites of MT nucleation. The reduced expression of TMBP200 leading to reduced growth of spindle MTs is consistent with the role of TMBP200 in promoting spindle MT assembly. TMBP200 similar to Mini spindles appears to have a further role in promoting spindle bipolarity that may act to suppress ectopic nucleation through regulated MT instability (Shirasu-Hiza *et al.*, 2003).

More recently, Kawamura and Wasteneys (2008) tracked dynamic events of MTs comparing various parameters in *mor1* root cells at permissive and restrictive temperatures. They reported that MT plus ends at restrictive temperatures are less dynamic with reduced growth and shrinkage velocities and increased pausing events. They proposed a modified working model in which MOR1 processively polymerizes the MT plus end as proposed by Brouhard *et al.* (2008), but with only the first TOG domain capturing a free tubulin dimer. Consequently, the other TOG domains in the N-terminus and the microtubule binding domain in the C-terminus are proposed to be dragged along in an inch-worm-like action along the MT lattice through partial dissociation stimulated by the higher affinity of the first TOG domain for free tubulin dimer.

These authors further reported that in *mor1-1* root cells at restrictive temperatures, MT plus ends showed reduced association with the plus end tracking protein EB1 as well as less dynamicity (Kawamura and Wasteneys, 2008). Therefore TMBP200-depletion could modulate molecular interactions required for spindle orientation control through direct or indirect interaction with EB1 or other proteins. In *Arabidopsis* suspension cells, Chan *et al.* (2005) showed that AtEB1α-GFP-labelling of MT plus ends at the nuclear periphery segregates into two polar caps before nuclear envelope breakdown and continuously marks the spindle poles. Dhonukshe *et al.* (2006) using tobacco BY-2 cells documented that GFP-AtEB1-labelled MT plus ends penetrate inside the nuclear envelope and form antiparallel bundles that subsequently define the spindle axis.

Currently there is no evidence for plant MAP215/Dis1 proteins interacting with EB1, however, it will be interesting to track EB1 localization in relation to the determination of spindle orientation by further exploiting these marker lines. Obvious differences between somatic and gametophytic cells in their requirement for the PPB in division plane determination may imply additional cofactors that enable plant MAP215/Dis1 proteins to promote the organization of cell type-specific MT arrays.

Acknowledgements

We thank Seiichiro Hasezawa for providing the Pro35S:GFP-TUA6 construct, Stefan Hyman and Natalie Allcock (University of Leicester, Electron Microscope Laboratory) for expert help with electron microscopy, and Graham Benskin and June Saddington for greenhouse assistance. This work was supported by grant funding from the Biotechnology and Biological Research Council to DT (BBSRC 91/18532, BB/E001017/1). SAO was supported by the Korea Research Foundation Grant funded by the Korean Government (KRF-F00008). SKP was supported by a grant from the Korea Research Foundation by the Korean Government (KRF-C00849).

References

Abe T, Hashimoto T. 2005. Altered microtubule dynamics by expression of modified α-tubulin protein causes right-handed helical

growth in transgenic Arabidopsis plants. *The Plant Journal* **43,** 191–204.

Borg M, Brownfield L, Twell D. 2009. Male gametophyte development: a molecular perspective. *Journal of Experimental Botany* **60,** 1465–1478.

Brouhard GJ, Stear JH, Noetzel TL, Al-Bassam J, Kinoshita K, Harrison SC, Howard J, Hyman AA. 2008. XMAP215 is a processive microtubule polymerase. *Cell* **132,** 79–88.

Brownfield L, Hafidh S, Borg M, Sidorova A, Mori T, Twell D. 2009. A plant germline-specific integrator of sperm specification and cell cycle progression. *PLoS Genetics* 5, e1000430.

Burk DH, Zhong R, Morrison III WH, Ye ZH. 2006. Disruption of cortical microtubules by overexpression of green fluorescent protein-tagged α-tubulin 6 causes a marked reduction in cell wall synthesis. *Journal of Integrative Plant Biology* **48,** 85–98.

Chan J, Calder G, Fox S, Llyod C. 2005. Localization of the microtubule end binding protein EB1 reveals alternative pathways of spindle development in Arabidopsis suspension cells. *The Plant Cell* **17,** 1737–1748.

Custers JBM, Oldenhof MT, Schrauwen JAM, Cordewender JHG, Wullems GJ, van Lookeren Campagne MM. 1997. Analysis of microspore-specific promoters in transgenic tobacco. *Plant Molecular Biology* **35,** 689–699.

Dhonukshe P, Vischer N, Gadella Jr TWJ. 2006. Contribution of microtubule growth polarity and flux to spindle assembly and functioning in plant cells. *Journal of Cell Science* **119,** 3193–3205.

Dumas C, Berger F, Faure JE, Matthys-Rochon E. 1998. Gametes, fertilization and early embryogenesis in flowering plants. *Advances in Botanical Research* **28,** 231–261.

Eady C, Lindsey K, Twell D. 1995. The significance of microspore division and division asymmetry for vegetative cell-specific transcription and generative cell differentiation. *The Plant Cell* **7,** 65–74.

Eleftheriou EP, Baskin TI, Hepler PK. 2005. Aberrant cell plate formation in the *Arabidopsis thaliana microtubule organzation 1* mutant. *Plant and Cell Physiology* **46,** 671–675.

Gard DL, Becker BE, Rommey SJ. 2004. MAPping the eukaryotic tree of life: structure, function, and evolution of the MAP215/Dis1 family of microtubule-associated proteins. *International Review of Cytology* **239,** 179–272.

Gard DL, Kirschner MW. 1987. A microtubule-associated protein from *Xenopus* eggs that specifically promotes assembly at the plus end. *Journal of Cell Biology* **105,** 2203–2215.

Gusti A, Baumberger N, Nowack M, Pusch S, Eisler H, Potuschak T, De Veylder L, Schnittger A, Genschik P. 2009. The *Arabidopsis thaliana* F-Box protein FBL17 is essential for progression through the second mitosis during pollen development. *PLoS ONE* **4,** e4780.

Hamada T, Igarashi H, Itoh TJ, Shimmen T, Sonobe S. 2004. Characterization of a 200 kDa, microtubule-associated protein of tobacco BY-2 cells, a member of the XMAP215/MOR1 family. *Plant and Cell Physiology* **45,** 1233–1242.

Kawamura E, Himmelspach R, Rashbrooke MC, Whittington AT, Gale KR, Collings DA, Wasteneys GO. 2006. *MICROTUBULE ORGANIZATION 1* regulates structure and function of microtubule arrays during mitosis and cytokinesis in the *Arabidopsis* root. *Plant Physiology* **140,** 102–114.

Kawamura E, Wasteneys GO. 2008. MOR1, the *Arabidopsis thaliana* homologue of *Xenopus* MAP215, promotes rapid growth and shrinkage, and suppresses the pausing of microtubule *in vivo*. *Journal of Cell Science* **121,** 4114–4123.

Kim HJ, Oh SA, Brownfield L, Hong SH, Ryu H, Hwang I, Twell D, Nam HG. 2008. Control of plant germline proliferation by SCF(FBL17) degradation of cell cycle inhibitors. *Nature* **455,** 1134–1137.

Lalanne E, Twell D. 2002. Genetic control of male germ unit organization in Arabidopsis. *Plant Physiology* **129,** 865–875.

Lucas JR, Nadeau JA, Sack FD. 2006. Microtubule arrays and *Arabidopsis* stomatal development. *Journal of Experimental Botany* **57,** 71–79.

McCormick S. 2004. Control of male gametophyte development. *The Plant Cell* **16,** Supplement S142–S153.

Muller S, Wright AJ, Smith LG. 2009. Division plane control in plants: new players in the band. *Trends in Cell Biology* **19,** 180–188.

Ohkura H, Adachi Y, Kinoshita N, Niwa O, Toda T, Yanagida M. 1988. Cold-sensitive and caffeine-supersensitive mutants of the *Schizosaccharomyces pombe dis* genes implicated in sister chromatid separation during mitosis. *EMBO Journal* **7,** 1465–1473.

Park SK, Howden R, Twell D. 1998. The *Arabidopsis thaliana* gametophytic mutant gemini pollen disrupts microspore polarity, division asymmetry and pollen cell fate. *Development* **125,** 3789–3799.

Park SK, Twell D. 2001. Novel patterns of ectopic cell plate growth and lipid body distribution in the Arabidopsis *gemini pollen1* mutant. *Plant Physiology* **126,** 899–909.

Sanger JM, Jackson WT. 1971. Fine structure study of pollen development in *Haemanthus katherinae* Baker. *Journal of Cell Science* **8,** 303–315.

Shirasu-Hiza M, Coughlin P, Mitchison T. 2003. Identification of XMAP215 as a microtubule-destabilizing factor in *Xenopus* egg extract by biochemical purification. *Journal of Cell Biology* **161,** 349–358.

Tanaka I, Nakamura S, Miki-Hirosige H. 1989. Structural features of isolated generative cells and their protoplasts from pollen of some liliaceous plants. *Gamete Research* **24,** 361–374.

Terasaka O, Niitsu T. 1987. Unequal cell division and chromatin differentiation in pollen grain cells. I. Centrifugal, cold and caffeine treatments. *The Botanical Magazine Tokyo* **100,** 205–216.

Terasaka O, Niitsu T. 1995. The mitotic apparatus during microspore division observed by a confocal laser scaning microscope. *Protoplasma* **189,** 187–193.

Theunis CH, Pierson ES, Cresti M. 1992. The microtubule cytoskeleton and the rounding of isolated generative cells on *Nicotiana tabacum*. *Sexual Plant Reproduction* **8,** 70–76.

Twell D, Park SK, Lalanne E. 1998. Asymmetric division and cell-fate determination in developing pollen. *Trends in Plant Sciences* **3,** 305–310.

Twell D, Park SK, Hawkins TJ, Schubert D, Schmidt R, Smertenko A, Hussey PJ. 2002. MOR1/GEM1 has an essential role in the plant-specific cytokinetic phragmoplast. *Nature Cell Biology* **4,** 711–714.

Ueda K, Matsuyama T, Hashimoto T. 1999. Visualisation of microtubules in living cells of transgenic *Arabidopsis thaliana*. *Protoplasma* **206,** 201–206.

Wasteneys GO, Yang Z. 2004. New views on the plant cytoskeleton. *Plant Physiology* **136,** 3884–3891.

Whittington AT, Vugrek O, Wei KJ, Hasenbein NG, Sugimoto K, Rashbrooke MC, Wasteneys GO. 2001. MOR1 is essential for organizing cortical microtubules in plants. *Nature* **411,** 610–613.

Yasuhara H, Muraoka M, Shogaki H, Mori H, Sonobe S. 2002. TMBP200, a microtubule bundling polypeptide isolated from telophase tobacco BY-2 cells is a MOR1 homologue. *Plant and Cell Physiology* **43,** 595–603.

Zonia L, Tupy J, Staiger CJ. 1999. Unique actin and microtubule arrays co-ordinate the differentiation of microspores to mature pollen in *Nicotiana tabacum*. *Journal of Experimental Botany* **50,** 581–594.